TRACK-BASED MUON SYSTEM ALIGNMENT AT CMS

An Undergraduate Research Scholars Thesis

by

GREYSON NEWTON[1]

Submitted to the LAUNCH: Undergraduate Research office at
Texas A&M University
in partial fulfillment of the requirements for the designation as an

UNDERGRADUATE RESEARCH SCHOLAR

Approved by
Faculty Research Advisor : Dr. Teruki Kamon

May 2021

Major: Physics[1]

RESEARCH COMPLIANCE CERTIFICATION

Research activities involving the use of human subjects, vertebrate animals, and/or biohazards must be reviewed and approved by the appropriate Texas A&M University regulatory research committee (i.e., IRB, IACUC, IBC) before the activity can commence. This requirement applies to activities conducted at Texas A&M and to activities conducted at non-Texas A&M facilities or institutions. In both cases, students are responsible for working with the relevant Texas A&M research compliance program to ensure and document that all Texas A&M compliance obligations are met before the study begins.

I, Greyson Newton[1], certify that all research compliance requirements related to this Undergraduate Research Scholars thesis have been addressed with my Research Faculty Advisor prior to the collection of any data used in this final thesis submission.

This project did not require approval from the Texas A&M University Research Compliance & Biosafety office.

TABLE OF CONTENTS

Page

ABSTRACT 1

ACKNOWLEDGMENTS 2

NOMENCLATURE 3

CHAPTERS

1. INTRODUCTION 4

    1.1 Large Hadron Collider (LHC) 4
    1.2 The CMS Experiment 6
    1.3 CMS Muon System 8

2. TRACK-BASED MUON ALIGNMENT 10

    2.1 Geometry 10
    2.2 Reconstruction 12
    2.3 Alignment Algorithms 13
    2.4 Statistical and Systematic Uncertainties 16
    2.5 CSC Disk Alignment 16
    2.6 Results 18

3. PHYSICS VALIDATION 19

4. SUMMARY 21

REFERENCES 22

ABSTRACT

Track-Based Muon System Alignment at CMS

Greyson Newton[1]
Department of Physics[1]]
Texas A&M University

Research Faculty Advisor: Dr. Teruki Kamon
Department of Physics
Texas A&M University

Track-Based Alignment of the CMS Muon System - Muon detection and reconstruction at the CMS experiment relies upon synchronized alignment between the Muon System and the Tracker System. Misalignment of these two systems will invalidate any new possible particle discoveries at the LHC. A set of algorithms have been created that detect misalignments as small as 300 μm and adjust collision data based upon the misalignment. This alignment process is fundamental to the functioning of the CMS experiment at the LHC. Therefore, this paper will serve as an analysis of Track-Based Muon Alignment and will help document the effective union between advanced computer science and physics.

ACKNOWLEDGMENTS

Contributors

I would like to thank my faculty advisor, Dr. Kamon, and mentors Hyunyong Kim, and Ryan Mueller for their guidance and support throughout the course of this research.

Thanks also go to my friends and colleagues and the department faculty and staff for making my time at Texas A&M University a great experience.

Finally, thanks to my family and friends for their encouragement, patience and love.

The data sets analyzed for Track-Based Muon System Alignment were provided by CERN. The analyses depicted in Track-Based Muon System Alignment were conducted in part by CERN at Texas A&M University and is planned to be published.

All other work conducted for the thesis was completed by the student independently.

Funding Sources

Undergraduate research was free of funding.

NOMENCLATURE

TAMU	Texas A&M University
LHC	Large Hadron Collider
CERN	European Council for Nuclear Research
SM	Standard Model
CMS	Compact Muon Solenoid
TBMA	Track-Based Muon Alignment

1. INTRODUCTION

1.1 Large Hadron Collider (LHC)

CERN stands for "*Conseil Européen pour la Recherche Nucléaire*", or the European Council for Nuclear Research, and is currently one of the world's largest and well-respected centers for physics research. CERN origins can be traced all the way back to the 1940's, when an initial group of scientists identified the need for Europe to develop a globally collaborative physics centre focused on peaceful post WWII physics and engineering [1]. CERN was officially signed into existence in 1953 by 12 founding European states, which in time would massively expand to 23 member-states (European countries) and many major non-member states, including: Japan, Australia, United States, Russia. As of 2017 there were 17,500 people collaborating with CERN, 2,500 of which work on the physical research infrastructure at CERN's the Large Hadron Collider (LHC), the world's largest and most powerful particle accelerator[2]. Below, Fig. 1.1 helps visualize the LHC.

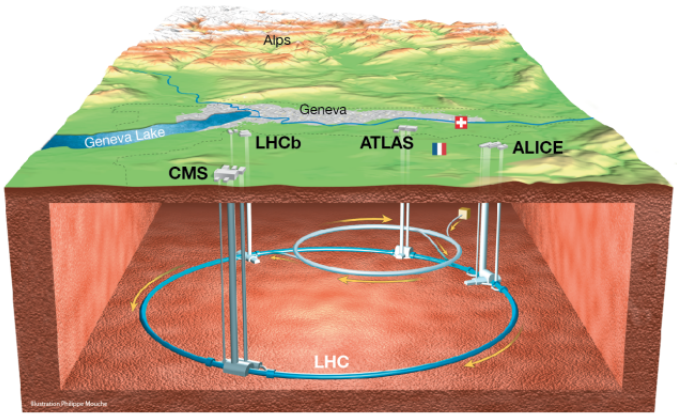

Figure 1.1: The LHC, pictured above, consists of rings of electromagnetic superconductors that magnetically accelerate two opposite traveling beams of protons to near the speed of near light and collide them at the center point of one of the detectors mentioned below.

Each major detector (CMS, ATLAS, LHCa (ALICE), LHCb) hosts their own experiments, and are independently operated by their own unique collaborations of scientists. The CMS and ATLAS detectors are the two biggest experiments, these two collaborations are responsible for corroborating any discovery the other experiment makes. For example, the newly discovered particle, Higg's, needed to be reliably observed, recorded and analyzed by both CMS and ATLAS before the findings could result in science accepting the existence of a new particle. Beyond CMS and ATLAS, the LHCa and LHCb work on specialty experiments and do not normally contribute on the same level as CMS or ATLAS. As a side note, the management of the CMS and ATLAS detectors is completely separated to allow CERN to validate any findings that come out of the LHC as a whole. This implies that most every process within these detectors need to be validated and held against any internal or external scrutiny [3].

Figure 1.2: The SM explains how the basic building blocks of matter(sub atomic particles) interact with each other, it looks like a variant of the periodic table.

Generally, these four detectors have taken data on billions of collisions since the LHC's first ever run in November 2009. The continuous operation time of the LHC is called 'Run 1' and spanned from 2009 to 2013. During the following "Long Shutdown" (LS1) from 2013 to 2015 maintenance and upgrades were made everywhere at the LHC. From 2015 to 2018 the LHC was in "Run 2" and during this time discovered the Higgs boson! As of the writing of this paper, was the last operational run. The current Long Shutdown (LS2) ends in March of 2021 opening the LHC up to Run 3 in 2021. The Higgs particle discussed above has been described by many physicists as the "God" particle because of its invaluable role in understanding particle physics through the Standard Model (SM). [Fig. 1.2]

1.2 The CMS Experiment

Texas A&M University (TAMU) works remotely with the CMS experiment at the LHC on maintaining an accurate alignment of the CMS's muon subsystem. TAMU achieves alignment through creating and maintain numerous proprietary algorithms that will be further explained as the Track-Based Muon Alignment (TBMA) process. Before TBMA is discussed, lets describe the specifics of CMS.

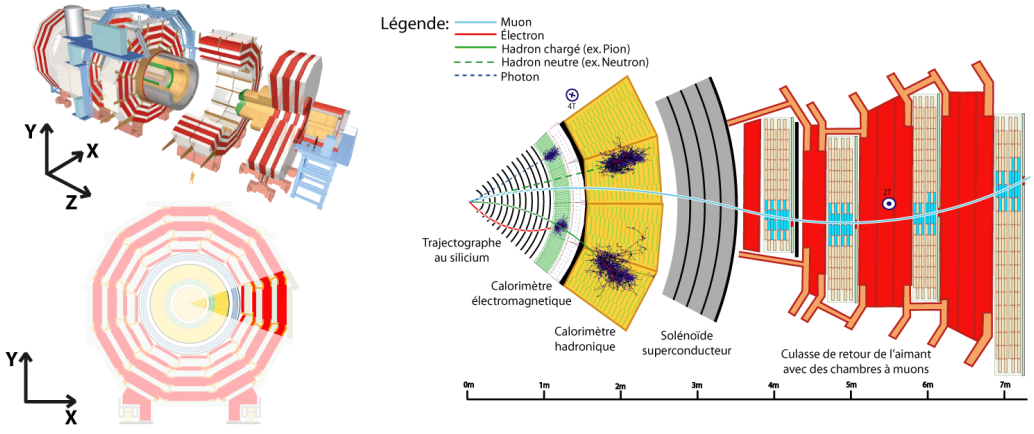

Figure 1.3: CMS is built around a gigantic cylindrical magnet that generates a magnetic field of 4 tesla - about 100,000 times the magnetic field of the Earth. The bulk of the detector's 14,000-tonnes comes from a steel "yoke" that contains this field. The complete detector is 21 metres long, 15 metres wide and 15 metres high [**?**].

CMS is a general-purpose detector at the LHC that utilizes its large magnetic field to better study muons, a subclass of sub-atomic particles, described by the SM. CMS uses particle data to search for extra dimensions, new exotic particles (Higgs!), and particles that could make up dark matter. Although the CMS and ATLAS experiments have similar scientific goals, ATLAS differs in technical solutions and a different magnet-system design [4]. The CMS detecting system is

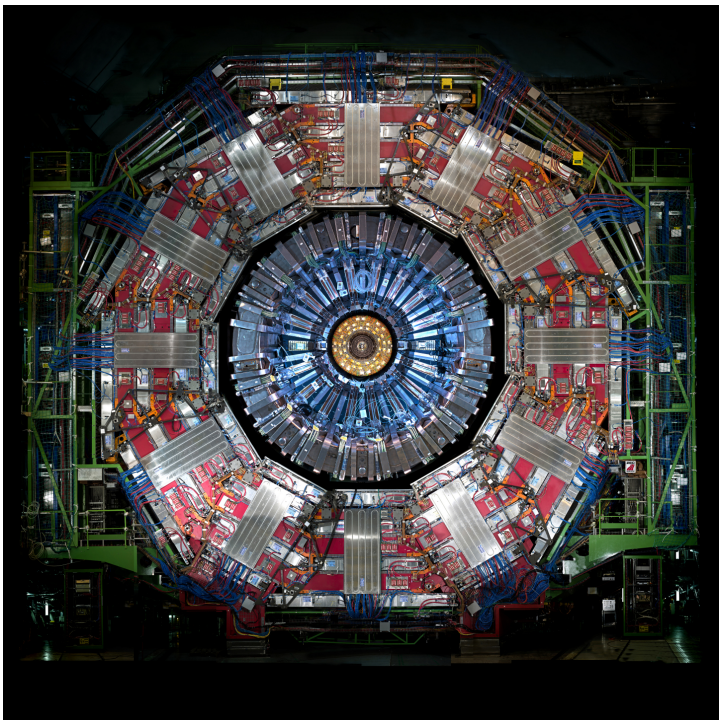

Figure 1.4: Cross section of the CMS Detector

built upon the collaboration between two complementary detector subsystems, the inner tracker system and the muon system. The inner tracker is outfitted with technology to detect and measure the kinematics of baryonic material, while the muon system is designed to trigger when in the presence of muons. At the LHC, muons are used to identify sensitive signatures of new and exotic particles. Therefore alignment of the muon detector system is one of the important operational tasks - ensuring stable trigger performance during data taking, and excellent muon reconstruction in physics analyses.

1.3 CMS Muon System

The CMS muon system consists of four types of gaseous ionization chambers: Drift Tube Chambers (DT's), Cathode Strip Chambers (CSC's), Resistive Plate Chambers (RPC's), and Gas Electron Multipliers (GEM's), as shown in Fig. 1.5. Reference [5, 6, 7, 8] for a detailed description of these chambers.

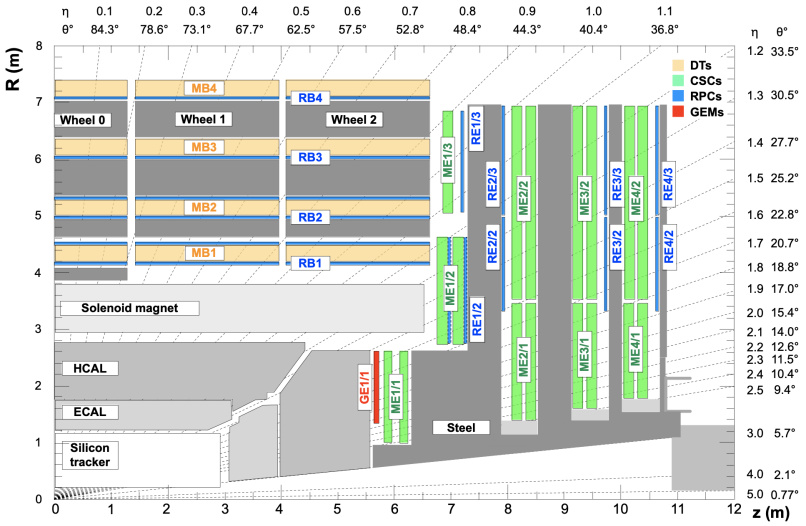

Figure 1.5: The CMS muon system for the $+\eta$ upper quadrant. DTs, CSCs, and RPCs in the muon system are highlighted.

DT chambers are found around the barrel, within the psuedorapidity region of $|\eta| < 1.2$. The DT chambers are broken up into 5 wheels, counting from -2 to 2, each wheel containing 4 stations numbered 1 to 4. On the other hand, CSC chambers are located within the psuedorapidity region of $0.9 < |\eta| < 2.4$ and are split into 4 stations, each with 2-3 rings. The muon system organization can be seen in Fig. 1.5.

The DT and CSC systems yield accurate measurements of the position and momentum of muons that cross between chamber boundaries while the RPC's primarily provide timing information for muon boundary triggers. DT's are located around the solenoid and CSC's cover the end-caps of the cylindrical solenoid. Muon hits detected in these chambers allow us to piece together a

time-dependent 3D graph of past events. It is actually common practice to simulate collisions that haven't been observed, allowing us to do research on new data even during long shutdowns.

2. TRACK-BASED MUON ALIGNMENT

All muon chamber positions (DT, CSC, GEM) are recorded at CERN, but overtime these chambers shift - creating a discrepancy between where we think the chambers are versus where they actually are. This is defined as "residual", or a difference between predicted and actual positions of chambers. Residuals in the chamber geometry results in recording inaccurate muon data, rendering valuable particle physics data useless. Therefore, misalignments of the muon subsystem compromise the integrity of any new particle discoveries at CMS. To preserve the accuracy of collected muon data, TAMU maintains a code-base that "aligns" muon chambers through analyzing shifts in muon chambers and then correcting chamber position and muon trajectory data based on the measured misalignments. The code-base that TAMU is responsible for maintaining is named Track Based Muon Alignment (TBMA) and will be discussed further below.

2.1 Geometry

In this section, we will briefly discuss the coordinate systems necessary to understand TBMA. The global CMS coordinate system has cylindrical coordinates due to the detector geometry, and defines position throughout the detector using this coordinate system, (x,y,z,ϕ,θ). The diagram in Fig. 2.1 represents the CMS global coordinate system.

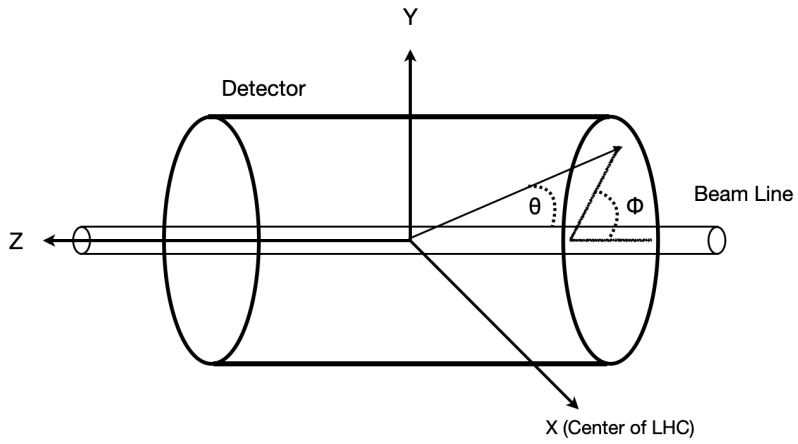

Figure 2.1: The CMS experiment uses a right-handed global coordinate system centered at the interaction point

Local coordinate systems for both DT and CSC geometries are defined and nested inside the above global coordinates [Fig 2.2]. The local coordinate system used for DT's and CSC's is in the

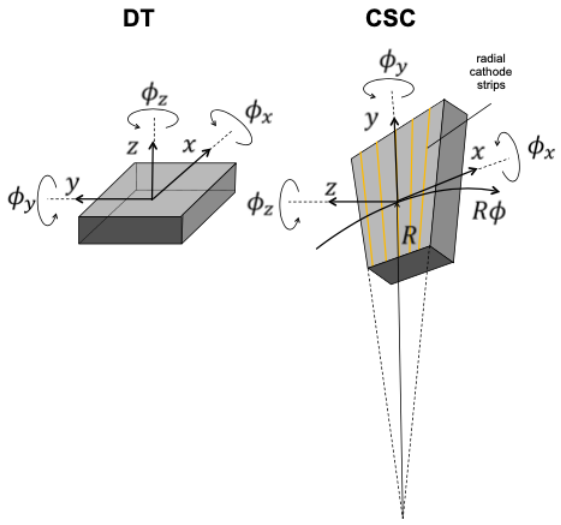

Figure 2.2: The muon subsystem uses two local coordinate systems with the origins resting in the center of a chamber.

Cartesian form of (x,y,z). However, CSC's have a radial aspect to their geometry, and therefore we measure $R\phi$ instead of local x for CSC's. From these coordinate system we can define a chamber's different degrees of freedom (DOF). The DOF of a chamber also describes the different directions that a chamber can be misaligned or shifted in. The total possible chamber misalignment directions is defined by the vector, $\mathbf{p}_{total} = \{\delta x, \delta y, \delta z, \delta\phi_x, \delta\phi_y, \delta\phi_z\}$.

2.2 Reconstruction

A muon track consists of a set of recorded hits from both the inner tracker system and the muon chamber system. A muon trajectory is extrapolated from the recorded hits contained in the muon track and serves to define the exact path of the muon candidate. To avoid potential biases the muon system, only tracks with both inner tracker and muon hits are used to generate a muon candidate's trajectory.

Table 2.1: Summary of muon data selection criteria.

Muon Selection	**Criteria**
Transverse Momentum(p_T)	30 GeV $< p_T <$ 200 GeV
Pseudorapidity (η)	$\lvert\eta\rvert <$ 2.4
Muon Track Selection	**Criteria**
Minimum number of inner tracker hits	10
Minimum number of matched muon stations	2
Maximum χ^2 (normalized by number of DOF)	10
Maximum track impact parameters (D_{xy})	0.2

High quality muon tracks are needed in order to start the TBMA process. Muons with transverse momenta between $30 < p_T < 200$ GeV are selected to avoid muon scattering. To ensure that the muon track originated from the interaction point and has enough inner tracker data, the muons must have at least ten inner tracker hits, a normalized $\chi^2 < 10$ (error in track reconstruction), and be matched with two or more muon stations. Finally, fiducial cuts are placed around muon

chamber boundaries to clarify what hits belong to what chambers, a summary of these filters is provided above in Table 2.1.

2.3 Alignment Algorithms

Muon tracks that pass the selection process are run through a series of reference target algorithms that calculate misalignments present in each chamber's DOF [5]. This is done through constructing the global multidimensional objective function found in Eq. 1 that sums over each chamber's residual probability distribution.

$$L_{global} = \sum_{l} \sum_{k} L_{kl}(x^0_{kl}, \sigma_k \mid x_{kl}) \qquad \text{(Eq. 1)}$$

where σ_k is a nuisance parameter, x_{kl} and x^0_{kl} are the measured and expected muon track parameters for each calculable residual type(k) and for every muon track(l). It is assumed that x_{kl} is a normal distribution that naturally centers around x^0_{kl} if the chamber is aligned. The different residual types, for example, could be for a hit position or track slope. The log-likelihood of a measured hit detected in a chamber is defined below.

$$L_{kl}(x^0_{kl}, \sigma_k \mid x_{kl}) = -\frac{(x_{kl} - x^0_{kl})^2}{2\sigma_k^2} - \frac{1}{2} ln 2\pi - ln\sigma_k \qquad \text{(Eq. 2)}$$

The log-likelihood function above essentially outputs the most probable residual found for the given chamber. A residual is defined as $\Delta_{kl} = (x_{kl} - x^0_{kl})$ and is visually illustrated in Fig. 2.3.

Also, the type of residual differs depending on the the local coordinate system of that chamber layer's geometry. For DT's, the local geometry is in regular Cartesian coordinates, giving layer-level residuals in the form of Δx and Δy. The local coordinate system for CSC's is defined using r and ϕ, therefore layer-level residuals take the form, Δ(Rϕ).

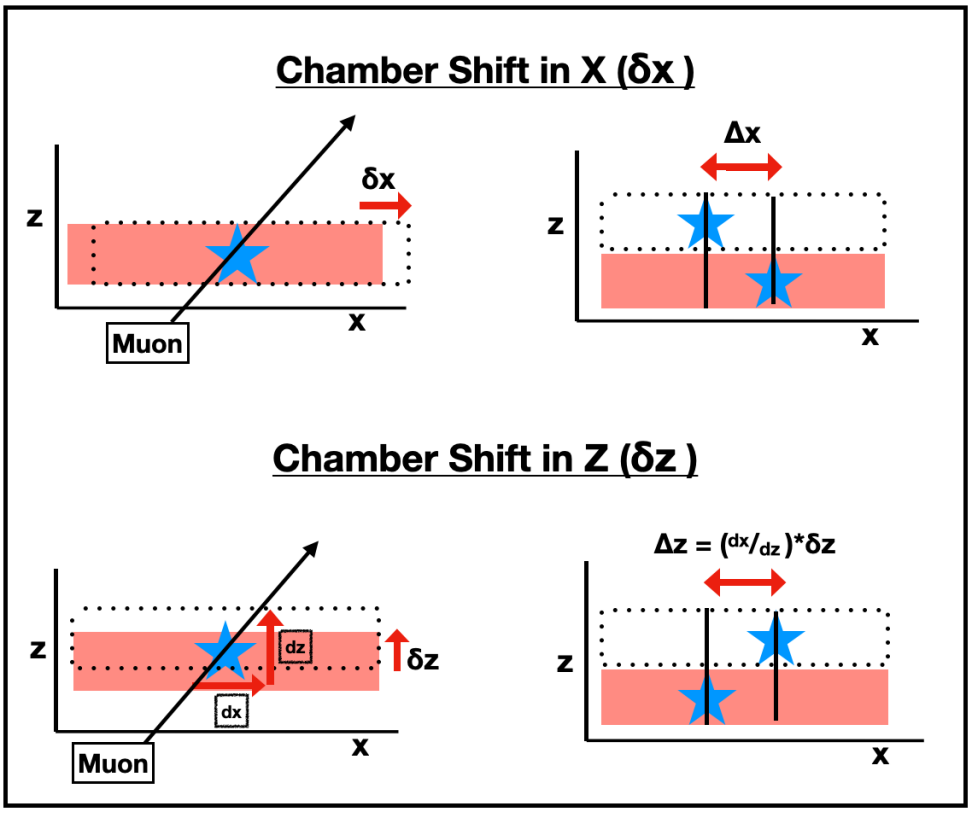

Figure 2.3: ΔX residual contributions from chamber misalignments in the x (top) and z (bottom) directions (δx, δz). Shifts in the y axis (δy) are not shown due to chamber displacements in the y direction having no effect on Δx residual calculation. The muon trajectory slope ($\frac{dx}{dz}$) is used to correct for distance the muon traveled in the x direction while flying through the chamber in the z direction.

The calculation of a chamber's residual is dependent off of the misalignment of the individual layers inside. Each layer gets analyzed for residuals and the resulting set of layer-level residuals are then used as input to calculate the encompassing chamber-level residual. Eq. 2 describes the relationship between chamber misalignment parameters, $\mathbf{p}_{total} = \{\delta x, \delta y, \delta z, \delta\phi_x, \delta\phi_y, \delta\phi_z\}$ and chamber residuals ($\mathbf{\Delta}$).

$$\mathbf{\Delta} = M\mathbf{p} \qquad \text{(Eq. 3)}$$

Where M is defined as the correlation matrix and contains local geometry information for either DT's or CSC's. For DT chambers, Δx and Δy layer-residuals are used along with residuals cal-

culated from the muon track slope, $\Delta\frac{dx}{dz}$ and $\Delta\frac{dy}{dz}$. The full relationship between DT residuals and chamber misalignment is described by the equation below.

$$\begin{pmatrix} \Delta x \\ \Delta y \\ \Delta\frac{dx}{dz} \\ \Delta\frac{dy}{dz} \end{pmatrix} = \begin{pmatrix} 1 & 0 & -\frac{dx}{dz} & -y\frac{dx}{dz} & x\frac{dx}{dz} & -y \\ 0 & 1 & -\frac{dy}{dz} & -y\frac{dy}{dz} & x\frac{dy}{dz} & x \\ 0 & 0 & 0 & -\frac{dx}{dz} & 1+(\frac{dx}{dz})^2 & -\frac{dy}{dz} \\ 0 & 0 & 0 & -1-(\frac{dy}{dz})^2 & \frac{dy}{dz}\frac{dx}{dz} & \frac{dx}{dz} \end{pmatrix} \begin{pmatrix} \delta x \\ \delta y \\ \delta z \\ \delta\phi_x \\ \delta\phi_y \\ \delta\phi_z \end{pmatrix} \quad \text{(Eq. 4)}$$

Fig. 2.3 visually illustrates an example of how misalignments in the x and y direction of DT chambers affect the DT Δ x residual calculation. For CSC chamber residual calculation, the local layer residual - $\Delta(R\phi)$ and the muon slope residual - Δd$(R\phi)$ are used. Δy residuals are precluded for CSCs due to inherent geometrical challenges in measurement. Eq. 4 describes the CSC residual-misalignment correlation.

$$\begin{pmatrix} \Delta(R\phi)) \\ \Delta y \\ \Delta\frac{d(R\phi)}{dz} \\ \Delta\frac{dy}{dz} \end{pmatrix} = \begin{pmatrix} 1 & [-\frac{x}{R}+3(\frac{x}{R})^3] & -\frac{dx}{dz} & -y\frac{dx}{dz} & x\frac{dx}{dz} & -y \\ 0 & 1 & -\frac{dy}{dz} & -y\frac{dy}{dz} & x\frac{dy}{dz} & x \\ 0 & \frac{1}{2R}\frac{dx}{dz} & 0 & [\frac{x}{R}-\frac{dy}{dz}\frac{dx}{dz}] & 1+(\frac{dx}{dz})^2 & -\frac{dy}{dz} \\ 0 & 0 & 0 & -1-(\frac{dy}{dz})^2 & \frac{dy}{dz}\frac{dx}{dz} & \frac{dx}{dz} \end{pmatrix} \begin{pmatrix} \delta x \\ \delta y \\ \delta z \\ \delta\phi_x \\ \delta\phi_y \\ \delta\phi_z \end{pmatrix} \quad \text{(Eq. 5)}$$

The next step in the alignment procedure is to effectively pass the calculated CSC and DT residuals and muon trajectories through a minimizer, MINUIT [9]. The global minimum of the alignment function contains a vector of the most probable chamber misalignments that is used to correct misaligned chamber positions. This process is repeated as many times as needed to attain an aligned chamber geometry.

2.4 Statistical and Systematic Uncertainties

Inherent differences in the sensitivities among chamber subgroups force us to model the total uncertainty as a convolution between systematic and statistical gaussian uncertainties, shown below.

$$\sigma_{total}(N) = \sqrt{\sigma_{syst}^2 + \frac{c_{stat}^2}{N}} \qquad \text{(Eq. 1)}$$

Where σ_{syst} is the systematic error and $\sigma_{syst} = \frac{c_{stat}^2}{\sqrt{N}}$ is the statistical error which depends on the number of muon segments N in each chamber. To provide an estimate of the systematic piece, we perform alignment with monte carlo (MC) data using a single-muon event generator in conjunction with a full simulation of muon scattering and detector response, and we choose an ideal muon geometry as the reference geometry (with all chambers at their local origins). Since the ideal geometry has no true misalignments, the result of the alignment reveals any systematics inherent to the alignment algorithm which show up as non-zero misalignments in this scenario. These misalignments are then interpreted as the systematic uncertainties.

2.5 CSC Disk Alignment

The procedure used to correct CSC disk-level misalignments will be discussed in this section. Disk-level shifts in CSC endcaps occur each time the endcaps are opened, creating a global misalignment in the CSC subsystem. Global shifts in the CSC subsystem result in a sinusoidal residual distribution across the disk and is visualized by the $R\phi$ residual versus global ϕ relationship in Fig. 2.5 (left). Global shifts occur in the muon system due to a variety of reasons, however each time the muon system is open or closed each CSC chamber experiences a very similar displacement in global position. This disk-shift example produces a sinusoidal R versus$R\phi$ residual distribution seen in the left plot of Fig. 2.5. The disk alignment can be performed through combining both global and local alignment procedures, the two step process shown in Fig. 2.4 illustrates this idea.

In this situation we measure global x and y relative to the global disk misalignment. The first

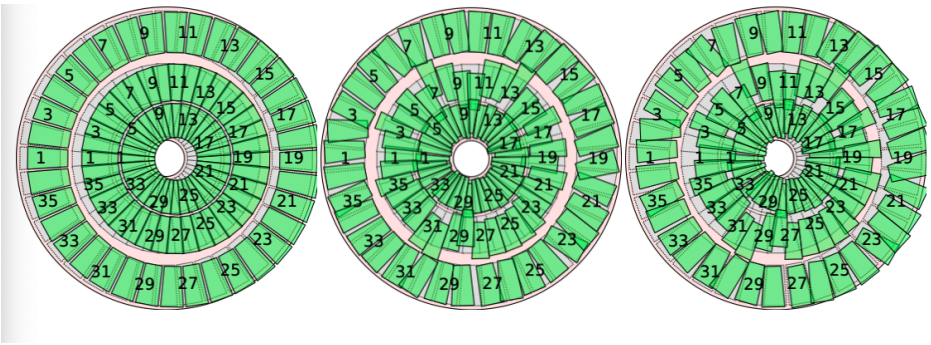

Figure 2.4: Two-step process of CSC ME+1/1 disk alignment. The image on the far left shows the results of a disk level alignment, the figure in the middle uses this updated disk geometry as a reference to perform chamber-level alignment. The final disk on the right shows the superposition of chamber movements generated through both alignment steps with respect to the original geometry. Chamber displacements have been scaled by a factor of 200.

CSC ring, ME+1/1 is analyzed due to having a higher data collection rate. The corrective shifts found for the first ring, however, get applied to the rest. The rightmost plot in Fig. 2.5 shows that after rings have been corrected, the sinusoidal residual trend disappears - illustrating the results of the TBMA procedure.

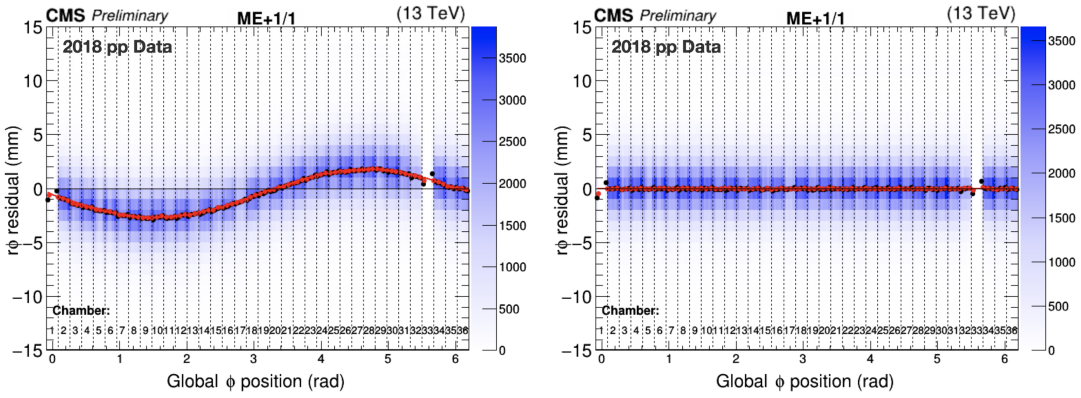

Figure 2.5: Residual on $R\phi$ as a function of global ϕ for the first ring on the first disk of the positive endcap. On the left, the residual distribution has a sinusoidal trend due to the misalignment of the CSC disk. On the right, the sinusoidal trend disappears once the initial geometry has been corrected.

2.6 Results

The results of performing the track-based muon alignment procedure will be discussed as a conclusion to this chapter on TBMA.

Track-based muon alignment, as described throughout this chapter, is an iterative process designed to be repeated several times in order to generate an aligned chamber geometry. When a new geometry is produced, it can be used for physics analysis throughout the CMS Collaboration. Aligned geometries do not last forever, they expire after the Interval Of Validity (IOV), which defines the period of time that a given geometry is or was used within the CMS system. Additionally, the TBMA procedure outputs Alignment Position Errors (APE's) as a part of the IOV. APE's contain chamber-level information on chamber alignment positioning errors.

The team behind TBMA at Texas A&M is proudly responsible for generating IOV's, which contributes to the overall study of particle physics at CMS.

3. PHYSICS VALIDATION

At the LHC, exotic particles have been found to sometimes decay into a pair of muons, the event is named a di-muon decay. These decays help detect hard to measure exotic particles, like the Z & W bosons. This is done through reconstructing muons paths accurately enough to piece together a picture of the undetectable particle that the muon pair originally decayed from. Excellent muon reconstruction requires the muon chamber system to be aligned within micrometers, TBMA specifically achieves alignment accuracies on the order of 300 μm.

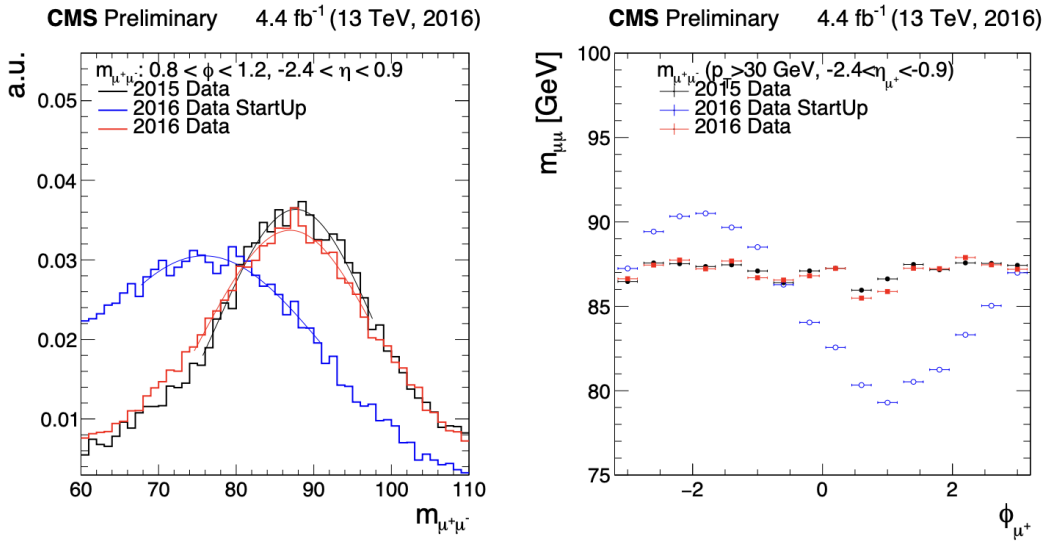

Figure 3.1: (Left) Di-muon mass peaks for muons between 0.8 $< \phi <$ 1.2. (Right) Mean of di-muon mass distributions vs ϕ, between -2.4 $< \phi <$ -0.9. The red distribution is calculated from an aligned and validated 2015 data set, whereas the blue and red distributions represent 2016 data collected before and after alignment (respectively).

Physics validation is the process of verifying the performance of TBMA. There several tests that contribute to validation, however one metric of interest, is the comparison between di-muon masses of this decay, $Z \rightarrow \mu^+\mu^-$. In order to begin validation analysis, trajectories of the di-muon decay are reconstructed within differing chamber geometries. Trajectory reconstruction is done through

mathematically modeling the measured mass and kinematics of the two muon paths, basing all calculations in whichever IOV that geometry belongs to. Di-muon mass and momenta distributions are extrapolated from these calculated di-muon trajectories. This implies a dependency between di-muon calculations and the geometry used when reconstructing the trajectories. We will analyze this dependency in order to understand how alignment accuracy is measured, and how physics validation of a geometry is achieved. Lets take a look at the 2015 and 2016 physics validation results found in above in Fig. 3.1.

Before alignment, the 2016 start-up distribution (blue) shows low measurement resolution (a small peak), and an inaccurate recording of the di-muon decay mass - unusable data. After alignment - a new 2016 geometry is created, represented in red and is compared to the 2015 validated di-muon mass distribution (black). The similarities between the red and black trends, help validate the 2016 TBMA process when compared to the inaccuracies of the initial 2016 geometry. Now, lets move to the other plot. Displayed on the right is the set di-muon momenta distributions constructed using the same geometric and track data as the left plot. The momenta plot highlights measurement improvements at high η. The sinusoidal behavior found in the initial geometry indicates a global misalignment of the muon system, as discussed in section 2.6. After comparing the 2015 validation geometry and the 2016 post-TBMA data, it is clear that the alignment process eliminates the global disk misalignment, conforming more to the black validation trend. The identical 2015 and 2016 post-TBMA distributions trends, in both plots, help confirm the results of the 2016 TBMA. Validation of TBMA as a process then, allows us to rely on the excellent reconstruction of muons and overal TBMA results. Therefore physics validation is mandatory to the alignment process.

4. SUMMARY

A description of CERN and the LHC has been made, along with a brief introduction to particle physics for context. Additionally, the role of Texas A&M to CMS particle physics was discussed through describing the processes that create the track-based muon alignment procedure. Walking through the alignment process, first TBMA is initialized with muon track data that passed the muon selection criteria. From this track data, trajectories were extrapolated and used to calculate chamber residual. The resulting residuals are passed through a minimzer, which outputs the most probable muon system misalignment scenario - down to 3/6 chamber degrees of freedom. With a residual description of the misaligned chamber geometry, corrective shifts are then applied in each DOF to each chamber or subgroup. This process repeats until the chamber geometry can be validated through physics validation. Run 2 physics validation was discussed using di-muon mass and momenta distribution relationships between a validated 2015 geometry and 2016 pre/post alignment geometries. Generally, this paper has investigated major aspects of TBMA and relayed important information on the current interesting and crucial particle physics research conducted at TAMU.

REFERENCES

[1] CERN - Accelerating Science, "Our History." Web, 2021. https://home.cern/about/who-we-are/our-history.

[2] CERN - Accelerating Science, "Our People." Web, 2021. https://home.cern/about/who-we-are/our-people.

[3] CERN - Accelerating Science, "CMS Experiment." Web, 2021. https://home.cern/science/experiments/cms.

[4] CMS Collaboration, "Detector." Web, 2021. https://home.cern/science/accelerators/large-hadron-collider.

[5] CMS Collaboration, "The CMS muon project : Technical Design Report," *Technical Report, CERN-LHCC-97-032, CMS-TDR-3, CERN, 1997*. http://cds.cern.ch/record/343814.

[6] CMS Collaboration, "CMS Physics : Technical Design Report Volume 1: Detector Performance and Software," *Technical Report CERN-LHCC-2006-001, CMS-TDR-008-1, CERN, 2006*. http://cds.cern.ch/record/922757.

[7] CMS Collaboration, "Performance of CMS muon reconstruction in pp collision events at $\sqrt{s}$ = 7 TeV," *JINST **7** (2012) P10002*. https://iopscience.iop.org/article/10.1088/1748-0221/7/10/P10002.

[8] CMS Collaboration, "Performance of CMS muon detector and muon reconstruction with proton-proton collisions at $\sqrt{s}$ = 7 TeV," *JINST **13** (2018) P06015*. https://iopscience.iop.org/article/10.1088/1748-0221/13/06/P06015.

[9] F. James and M. Roos, "Minuit: A System for Function Minimization and Analysis of the Parameter Errors and Correlations," *Comput. Phys. Commun. **10** (1975) 343–367*. https://doi.org/10.1016/0010-4655(75)90039-9.